



کد مقاله : ۲-۲۲۲۰-۱۰-A

تصویربرداری زیرطول موج چند مرحله‌ای مبتنی بر تمام‌نگاری

پوریا سلامی، لیلا یوسفی

تهران، خیابان کارگر شمالی، پردیس دانشکده‌های فنی دانشگاه تهران، دانشکده مهندسی برق و کامپیوتر

چکیده- برای دستیابی به تصویری با قدرت تفکیک فراتر از حد تفرق از یک جسم، لازم است تا بتوان از اطلاعات موجود در امواج میراشوندهی پراکنده شده از جسم نیز برای بازسازی تصویر استفاده کرد. در اینجا نشان داده می‌شود که در تکنیک تمام‌نگاری می‌توان با انجام چندین مرحله فرآیند بازسازی، اطلاعات موجود در محدوده وسیعی از امواج میراشوندهی پراکنده شده از جسم را برای بازیابی تصویر با قدرت تفکیک فراتر از حد تفرق، استفاده کرد. برای راستی‌آزمایی روش ارائه شده، با به کارگیری شبیه‌سازی تمام‌موج نشان داده می‌شود که با استفاده از انجام دو مرحله بازسازی در تکنیک ارائه شده، می‌توان به قدرت تفکیک فراتر از یک شانزدهم طول‌موج دست یافت.

کلیدواژه-تمام‌نگاری، تصویربرداری زیرطول‌موج، حد تفرق، تداخل

Multi-Step Holography-Based Super-Resolution Imaging

Pooria Salami, and Leila Yousefi

School of Electrical and Computer Engineering, College of Engineering, University of Tehran, Tehran 14395-515, Iran

Pooria.salami@ut.ac.ir, lyousefi@ut.ac.ir

Abstract-For achieving a super-resolution image of an object, it is necessary to use information included in evanescent waves scattered from the object, for image reconstruction. Here, we show that using multiple reconstruction processes in holography technique, we can extract information of a wide range evanescent waves scattered from the object, and we can use them for reconstructing an image with a resolution beyond the diffraction limit. In order to verify our proposed method, using full-wave numerical simulations and by applying two reconstruction processes, a resolution of one-sixteenth of the working wavelength is achieved.

Keywords: Holography, Sub-wavelength imaging, Diffraction limit, Interference.

1. Introduction

Waves scattered from an object, include both propagating and evanescent waves. Conventional optical imaging systems, such as ordinary microscopes, use only the propagating section of the scattered waves for image reconstruction [1]. This limits the resolution of the reconstructed image to about half of the wavelength, which is known as the diffraction limit [2]. In other words, information about sub-wavelength features of an object are embedded in the evanescent waves scattered from that object [3-4], and to achieve a sub-wavelength image, these information must be extracted from the evanescent waves.

Different methods have been proposed to convert evanescent waves into propagating modes and break the diffraction limit so far. Most of these methods are based on complex nano-structures [1,5-8], or fluorescent materials [9,10]. However, complexities in fabrication and using fluorescent materials, limit practical application of these methods [11].

In Ref. [12], we proposed a new sub-wavelength imaging method based on converting evanescent waves into propagating waves using holography. We showed that, super-resolution images of an object can be obtained without using complex nano-structures and fluorescent materials (a resolution of one-seventh of the working wavelength was achieved [12]). Here, we show both analytically and numerically that by using multiple reconstruction processes in holography-based sub-wavelength imaging technique, the resolution can be significantly improved. To verify our method, using full-wave numerical simulations and by applying two reconstruction processes, a resolution of one-sixteenth of the working wavelength is achieved.

2. Theory

The steps of the proposed technique have been shown in Fig. 1. In this technique, first, in step (a) the propagating section of the sample field

angular spectrum is detected using a conventional imaging system, with numerical aperture of $NA = 1$. This is equivalent to achieving information included in transverse wavenumbers of $[-k_0, k_0]$, where k_0 is the free space wavenumber. Then, in step (b), an emulsion (emulsion 1) is placed near the sample, and the interference of the sample field, $a(x)$, with a known evanescent reference wave, $A \exp(jk_{ref}x)$, is recorded on the emulsion (see Fig. 1(b)). Here, k_{ref} is the transverse wavenumber of the reference wave. Evanescent reference wave can be generated using total internal reflection concept. After developing emulsion 1, this interference intensity pattern results in transmittance of [12]:

$$t_a = t_b + \beta (|a(x)|^2 + A^* a(x) e^{-jk_{ref}x} + A a^*(x) e^{jk_{ref}x}), \quad (1)$$

where t_b and β are constants.

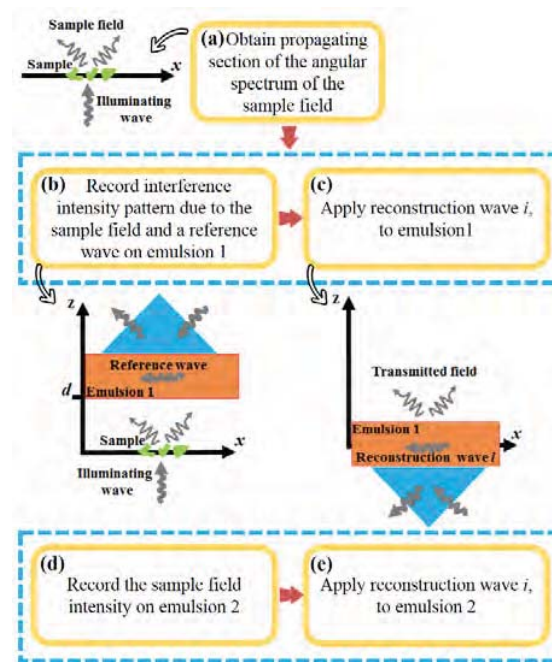


Fig. 1: Multi-step holography-based imaging.

Now, the evanescent reconstruction wave of $B \exp(j(2i+1)k_{ref}x)$ is applied to the emulsion 1 (where $i = 0, 1, 2, \dots$, shows the reconstruction stage number), as shown in Fig. 1(c), and the transmitted

field of, U_{ii} , is generated. This transmitted field can be written as:

$$U_{ii} = t_b B e^{j(2i+1)k_{ref} x} + \beta |a|^2 B e^{j(2i+1)k_{ref} x} + \beta B A a e^{j2ik_{ref} x} + \beta B A a e^{j2(i+1)k_{ref} x} \quad (2)$$

A similar equation can be obtained by reversing the direction of reference and reconstruction waves in steps (b) and (c) of Fig. 1. The first term in the right hand side of Eq. (2), shows an evanescent wave, and therefore does not exist in far-field region. However, the propagating section of the other three terms are present in far-field.

The last term of Eq. (2), shows a shift of $2(i+1)k_{ref}$, in the angular spectrum (Fourier space) of the sample field. In other words, a range of evanescent waves with transverse wavenumbers of $[2k_{ref}(i+1)-k_0, 2k_{ref}(i+1)+k_0]$ are transferred into propagating range, and their corresponding information can be detected in far-field region. By reversing the direction of reference and reconstruction waves, information of evanescent waves with transverse wavenumber of $[-k_0-2k_{ref}(i+1), k_0-2k_{ref}(i+1)]$ can also be detected in far-field. In fact, for different reconstruction waves (different i), each time a different range of evanescent waves are converted to propagating waves, and their information can be used for image reconstruction. However, these information must be separated from waves due to the second and third terms of Eq. (2).

To compute the propagating section of the angular spectrum of the second term in the right hand side of Eq. (2), steps (d) and (e) in Fig. 1, are performed. First, the intensity of the sample field (in the absence of the reference wave) is recorded on another emulsion (emulsion 2). Then the same reconstruction wave (i -th reconstruction wave) is applied to the developed emulsion (emulsion 2).

For calculating the propagating section of the third term of Eq. (2), a recursive relation is used. In the first step of the reconstruction process ($i = 0$), the third term is equivalent to $\beta B A a$, which in fact is a coefficient of the sample field. Therefore, propagating section of this term, is already known

from step (a) (see Fig. 1), using a conventional imaging system. At the end of the first reconstruction process and by solving Eq. (2), information included in evanescent waves scattered from the sample with transverse wavenumbers of $[2k_{ref}-k_0, 2k_{ref}+k_0]$ and $[-k_0-2k_{ref}, k_0-2k_{ref}]$, are obtained. In the second reconstruction process ($i = 1$), the third term in Eq. (2), is $\beta B A a \exp(j2k_{ref} x)$, which is known due to the results of the first reconstruction process. Therefore, by solving Eq. (2), this time information included in transverse wavenumbers of $[4k_{ref}-k_0, 4k_{ref}+k_0]$ and $[-k_0-4k_{ref}, k_0-4k_{ref}]$ are achieved. Repeating similar processes, in each reconstruction process, information of a different range of evanescent waves is obtained.

In next section, we use full-wave numerical simulations to validate our proposed method.

3. Numerical Simulation

3.1. Simulated Structure

In this section, based on numerical simulations, we use two reconstruction processes to achieve a sub-wavelength image of a sample. A schematic of the simulated structure is shown in Fig. 2. Here, two apertures in a PEC plane, are considered as the sample. The width of apertures and the gap between them are equal and shown by g in Fig. 2. The distance between the sample and the emulsion is chosen to be $d = 20$ nm. Ports 1 and 2 are used to generate gaussian illuminating and reference waves at wavelength of $\lambda = 400$ nm, respectively (see Fig. 1). Here, we use total internal reflection, to generate an evanescent reference wave with transverse wavenumber of $k_{ref} = 1.5k_0$. In this regard, the wave generated from port 2 (from a high refractive index medium), is incident on the emulsion with incidence angle of 45° . The refractive indices of the incident and refraction (emulsion) medium, are 2.12 and 1.49, respectively. It should be noted that we have used scattering boundary condition, for boundaries other than ports 1 and 2.

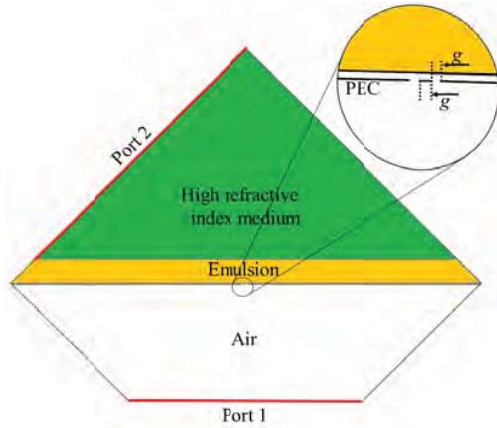


Fig. 2: Schematic of the simulated structure.

3.2. Simulation Results

The images achieved using one (dotted line) and two (dashed line) reconstruction processes for the case of $g = \lambda/16$, are shown in Fig. 3. These images are also compared with sample itself (field distribution 20 nm above the apertures), in Fig. 3. As is evident in this figure, using one reconstruction process, the apertures can not be resolved. However, using two reconstruction processes (using more evanescent waves), the apertures are resolved.

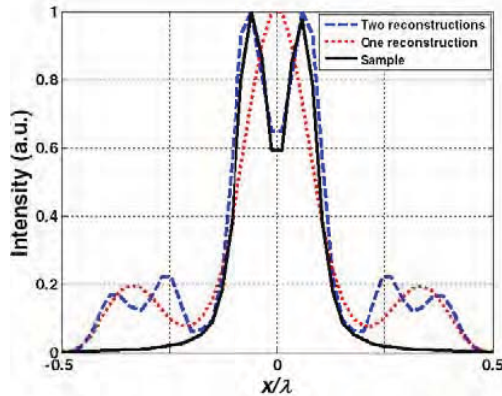


Fig. 3: Reconstructed images using proposed method.

4. Conclusion

Here, we proposed a multi-step holography-based sub-wavelength imaging method. We theoretically proved that using multiple reconstruction processes, information included in a wide range of

evanescent waves scattered from the sample, can be extracted. Moreover, using the proposed method and performing two reconstruction processes, a resolution of one-sixteenth of the working wavelength was obtained.

References

- [1] A. Salandrino and N. Engheta, "Far-field subdiffraction optical microscopy using metamaterial crystals: theory and simulations," *Phys. Rev. B*, Vol. 74, 2006.
- [2] M. Born and E. Wolf, *Principles of Optics*, 7th ed., Cambridge University Press, 1999.
- [3] J. W. Goodman, *Introduction to Fourier Optics*, 3rd ed., 2005.
- [4] J. B. Pendry, "Negative refraction makes a perfect lens," *Phys. Rev. Lett.*, Vol. 85, pp. 3966–3969, 2000.
- [5] S. Durant, Z. Liu, J. M. Steele, and X. Zhang, "Theory of transmission properties of an optical far-field superlens for imaging beyond the diffraction limit," *J. Opt. Soc. Am. B*, Vol. 23, pp. 2383–2392, 2006.
- [6] P. Salami and L. Yousefi, "Far field subwavelength imaging using phase gradient metasurfaces," *J. Lightw. Technol.*, Vol. 37, pp. 2317–2323, 2019.
- [7] P. Salami and L. Yousefi, "Evanescent-to-propagating wave conversion using plasmonic metasurfaces," 2018 Fifth International Conference on Millimeter-Wave and Terahertz Technologies (MMWaTT), 18-20 Dec. 2018, Tehran, Iran.
- [8] M. A. Shamsi, P. Salami, and L. Yousefi, "Light trapping in thin film solar cells using a polarization independent phase gradient metasurfaces," *J. Opt.*, Vol. 20, 2018.
- [9] M. J. Rust, M. Bates, and X. Zhuang, "Sub-diffraction-limit imaging by stochastic optical reconstruction microscopy (storm)," *Nat. Methods*, Vol. 3, pp. 793–796, 2006.
- [10] M. G. L. Gustafsson, "Surpassing the lateral resolution limit by a factor of two using structured illumination microscopy," *J. Microsc.*, Vol. 198, pp. 82–87, 2000.
- [11] M. Kim and J. Rho, "Metamaterials and imaging," *Nano Convergence*, Vol. 2, 2015.
- [12] P. Salami and L. Yousefi, "Far-field imaging beyond the diffraction limit using waves interference," *J. Lightw. Technol.*, Vol. 38, pp. 2322–2327, 2020.